

Statistical Tools for Analyzing the Cosmic Ray Energy Spectrum

J. D. Hague^{a,1} B. R. Becker^a M. S. Gold^a J.A.J. Matthews^a

^a *University of New Mexico, Department of Physics and Astronomy, Albuquerque, New Mexico, USA*

Abstract

In this paper un-binned statistical tools for analyzing the cosmic ray energy spectrum are developed and illustrated with a simulated data set. The methods are designed to extract accurate and precise model parameter estimators in the presence of statistical and systematic energy errors. Two robust methods are used to test for the presence of flux suppression at the highest energies: the Tail-Power statistic and a likelihood ratio test. Both tests give evidence of flux suppression in the simulated data. The tools presented can be generalized for use on any astrophysical data set where the power-law assumption is relevant and can be used to aid observational design.

Key words: cosmic ray spectrum, power-law, CRPropa, TP-statistic, flux suppression

1 Introduction

The observation of suppression in the flux of the highest energy cosmic rays (CRs) has been of central interest to astro-particle physics since the prediction of the GZK-effect[6,17] in 1966. Most recently both the Auger[15] and the HiRes[1] detectors have released results favoring the observation of flux suppression at a 6σ and 5σ level of confidence, respectively.

With this in mind, we describe a set of statistical tools designed to extract the most accurate and precise information concerning the flux of the highest energy cosmic rays. By binning the data we can only lose information[5] (see §A) and therefore our statistical tools use an un-binned maximum likelihood

¹ Corresponding author, E-mail: jhague@unm.edu

approach[16,9,11,4] to answer two related statistical questions: *Is there flux suppression at the highest energies?* and, if yes, *What are the characteristic cut-off energy and shape parameters?*

In detail we first generate a toy data set using the CRPropa package[2], as in §2.2. We then fit this simulated data to the three models described in §2.3. The un-binned maximum likelihood fit is outlined in §3.1 and methods for incorporating systematic and statistical energy errors are described in §3.2 and §3.3 respectively. In §4 we describe several statistical tools for hypothesis testing: the Kolmogorov-Smirnov test, the tail power statistic[12,7,15], and a likelihood ratio test[8].

Though we cast our discussion in terms of cosmic ray energies, it is worth noting that these tools can be applied to any astrophysical data set where deviations from the power-law hypothesis are relevant, e.g. the galaxy correlation function[18] or gamma ray astronomy[13].

2 CRPropa Data Set and Models

2.1 Input from the HiRes and Auger Observatories

Both the HiRes[1] and Auger[15] observatories have reported spectra and fit parameters for various power-law models. The collaborations use binned fitting methods. They fit the spectrum over many orders of magnitude in energy but we summarize here the model parameters² relevant only to the highest energies. The best fit double power-law parameters reported by HiRes[1] are $\gamma = 2.81 \pm 0.03(\text{stat}) \pm 0.02(\text{sys})$, $E_b = 10^{1.75 \pm 0.04}(\text{stat})$ and $\delta = 5.1 \pm 0.7(\text{stat})$. For the same model Auger[15] reports $\gamma = 2.62 \pm 0.03(\text{stat}) \pm 0.02(\text{sys})$, $E_b = 10^{1.6}(\text{fixed})$ and $\delta = 4.14 \pm 0.42(\text{stat})$. Fitting to the Fermi power-law Auger[15] finds $\gamma = 2.56 \pm 0.06(\text{stat})$, $E_{\frac{1}{2}} = 10^{1.74 \pm 0.06}(\text{stat})$ and $w_c = 0.16 \pm 0.04(\text{stat})$.

2.2 A Toy CR Data Set

To illustrate the methods in this note we use un-binned proton primary cosmic ray, CR, arrival energies (in EeV $\equiv 10^{18}\text{eV}$) as simulated by the package CRPropa[2] with input spectral index $\gamma_{\text{IN}} = 2.6$, $E_{\text{min}} = 10$ EeV and $E_{\text{max}} = 2000$ EeV. We draw 5×10^3 events to act as a *toy* data set from a modern CR detector.

² See §2.3 and Table 1 for the definition of these parameters.

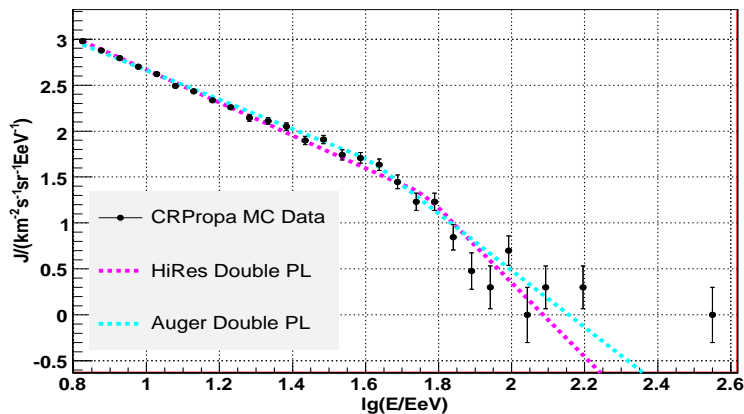


Fig. 1. The differential flux as simulated by 5×10^3 events from the CRPropa toy set with parameters $\gamma_{\text{IN}} = 2.6$ and $E_{\text{max}} = 2000$ EeV (see §2.2). The p.d.f. of the best fit double power-laws reported by HiRes[1] and Auger[15] are the dashed lines.

The CRPropa toy data set is similar size and shape to the flux reported by these observatories but the results of this study do not, otherwise, reflect any information about any physical data set. The probability distribution function (p.d.f.) of the best fit double power-laws reported by HiRes[1] and Auger[15] are shown in Fig.1 along with the CRPropa toy data.

The CRPropa propagation simulation is implemented by first generating proton CR primaries with initial energies according to a power-law “at the source,” propagating them through a simulated Universe and then observing the final energy. The spacial extent of the sources is simulated as a uniform distribution of discrete sources on a grid with 10 Mpc steps extending to a distance of 4.07 Gpc, (from redshift $z = 0.0$ to $z = 2.73$). Nuclei traveling over many megaparsecs from these sources will suffer significant energy loss in an expanding Universe filled with the cosmic microwave background, CMB, radiation. As a result, the highest energy flux is much less than one would expect from a power-law alone. This suppression is known as the GZK-effect[6,17].

2.3 Power-Law Models

The fundamental probability distribution function governing the pure power-law assumption, denoted f_{P} , is shown in Table 1: $f_{\text{P}} = (\gamma - 1)E_{\text{min}}^{\gamma-1}E^{-\gamma}$. The parameter γ is referred to as the *spectral index*. Here the sub-scripted-P stands for Pure-power-law.

For the highest energy CRs, the interesting observation would be to confirm or deny deviation from the power-law form at the highest magnitudes, i.e. the

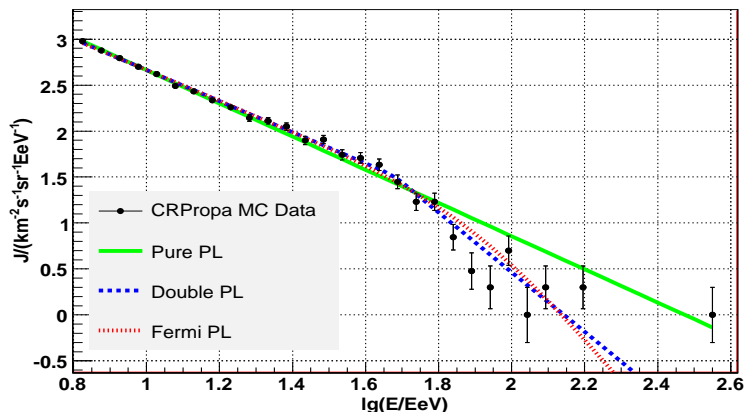


Fig. 2. The differential flux as simulated by 5×10^3 events from the CRPropa toy set with parameters $\gamma_{\text{IN}} = 2.6$ and $E_{\text{max}} = 2000$ EeV. The best fit models are described in §2.3.

GZK-cutoff. We therefore study two toy models that mimic a pure power-law for lower energies but exhibit flux suppression above a given energy. The first is a double power-law (DP) with two spectral indexes, γ below E_b (“b” for bend or break) and $\delta > \gamma$ above. The point at which this p.d.f. reaches half the value it would have if the pure power-law continued above E_b is given by $E_{\frac{1}{2}}^{\text{dp}} = 2^{\frac{1}{\delta-\gamma}} E_b$, see [3] for a discussion of this quantity. Both HiRes[1] and Auger[15] have analyzed their data using this model.

We also study a toy p.d.f. where the cut-off is a “Fermi-like” Power-law (FP)[15,7]. The advantage of fitting with this toy model is that the location parameter $E_{\frac{1}{2}}$ is a parameter in the fit.

All three p.d.f.’s are normalized on the interval $[E_{\text{min}}, \infty)$, i.e.

$\langle \rangle_M \equiv \int_{E_{\text{min}}}^{\infty} f_M(t) dt = 1$ for each of the models $M \in \{P, DP, FP\}$. The first element of the parameter vector $\theta_1 \equiv E_{\text{min}}$ is fixed for the fit (see §3) and then varied to estimate the stability (see §4.1). Thus the power-law has one free parameter and the other models have three; low energy spectral index, location of cut-off and “steepness” of cut-off.

3 Fitting the Data

We take an un-binned maximum log-likelihood approach to estimating the best-fit parameters of each model. The method constructed here is designed to extract the maximum possible statistical information about these parameters. For the ideal detector we assume that the observed energies are known with infinite precision.

Model	N_{dof}	Normalization	Function
P	1	$(\gamma - 1)E_{\text{min}}^{\gamma-1}$	$E^{-\gamma}$
DP	3	$\frac{\gamma-1}{E_b} \left\{ \left(\frac{E_b}{E_{\text{min}}} \right)^{\gamma-1} + \frac{\gamma-1}{\delta-1} - 1 \right\}^{-1}$	$\left(\frac{E}{E_b} \right)^{-\gamma} \quad E_{\text{min}} \leq E < E_b$ $\left(\frac{E}{E_b} \right)^{-\delta} \quad E_b \leq E$
FP	3	$\langle \rangle_{\text{FP}}^{-1}$, numerically	$E^{-\gamma} \left[1 + \left(\frac{E}{E_{\frac{1}{2}}} \right)^{1/(w_c \ln 10)} \right]^{-1}$

Table 1

The model designation (Model = Pure power-law, Double Power-law or Fermi Power-law), number of free parameters, normalization, and form of the function used to fit the simulated fluxes used in this study.

3.1 Ideal Detector

We find estimates of the parameters in each model by maximizing,

$$\mathcal{L}_M(\vec{\theta}) = \sum_{i=1}^N \ln \left\{ f_M(E_i; \vec{\theta}) \right\}, \quad (1)$$

where the sum is carried out over the event energies and $\theta_1 \equiv E_{\text{min}}$ is fixed. The global maximum of this function $\mathcal{L}_M(\hat{\theta})$ determines the best parameter estimates, $\hat{\theta}$. The the function is maximized using Minuit[10] with the MIGrad option.

To determine the one degree of freedom error estimate[16] for a parameter we vary the parameter (with the others fixed at $\hat{\theta}$) until $-2\Delta\mathcal{L}_M = 1$. The two degrees of freedom error estimates[16] are determined by varying two parameters with the other fixed and choosing the contour such that $-2\Delta\mathcal{L}_M \geq 2.3$. For the toy data set, we plot these contours and the asymmetric one degree of freedom error estimates in §C: Fig.C.3 and C.4.

3.2 Systematic Energy Error

The errors on the observed energy E_{obs} of an event from a real CR detector are considerable and must be included in any realistic analysis of a spectrum. For our purposes, these errors take the two canonical forms; *statistical* and *systematic*, i.e. $E_{\text{obs}} \pm \sigma_{\text{stat}} \pm \sigma_{\text{sys}}$.

The systematic errors energy errors of a CR detector reflect the uncertainties in the absolute calibration of the detector. At the highest energies the systematics are the dominant contribution to the overall uncertainty of an event's energy. For example, the two fluorescence detectors Auger[15] and Hires[1] re-

port uncertainties of 22% and 17% respectively.³ The shift in energy due to the systematic error can be asymmetric, i.e. $\sigma_{sys}^+ \neq \sigma_{sys}^-$, and energy dependent, see Eq(2), but it effects every event at a given energy the same way; a shift up or down. For the Monte-Carlo (MC) data sets we model the systematic detector energy errors using:

$$\frac{\sigma(E; \vec{p})}{E} = p_1 + p_2 \lg(E). \quad (2)$$

Here we choose symmetric systematically-shifted energies such that the energy of the k^{th} event is $E_k^\pm = E_k \pm \sigma(E_k; \vec{p}_{sys})$. For the systematic errors we choose $p_1 = 0.05$ and $p_2 = 0.10$.

To account for this in the parameter estimation procedure, we shift each energy up or down and carry out the methods in §3.1. The difference between the parameter estimates of a shifted set and those of the centered set gives “systematic” errors of the parameter estimates.

3.3 Statistical Energy Error

To model the statistical energy errors of the detector we assume that the *true* energy of the cosmic ray has a 68% chance of being within the interval $(E_{obs} - \sigma_{stat}, E_{obs} + \sigma_{stat})$. The observed energy has been “smeared” from the true value; $E_{obs} = E_{true} + Y$ where Y is drawn from a normal distribution with mean 0 and variance σ_{stat} . Note that while the true energies can only be found on $[E_{min}, \infty)$, there is a nonzero probability for the (after smearing) observed energy to be less than E_{min} ; E_{obs} lives on the interval $(-\infty, \infty)$. This edge effect near E_{min} can be accounted for by assuming that the true distribution of energies follows a power-law well below E_{min} and then re-normalizing the convolution technique used in Howell[9]. See §B for further discussion. For the integrand, three factors are necessary:

- (1) The model to be fitted, $f_M(t; \vec{\theta})$ (see §2.3). By letting $\theta_0 = 0.1E_{min}$ we are assuming that the power-law extends below the observed E_{min} .
- (2) A normal distribution $G(t; E_{obs}, \sigma_{stat}(t; \vec{p}))$ with mean E_{obs} and variance $\sigma_{stat}(t; \vec{p})$ to reflect the statistical energy errors.
- (3) The acceptance of the CR detector as a function of the true energies $\Omega(t)$. Since we are using MC data we choose $\Omega(t) = 1$ for simplicity.

³ With its hybrid detector the Auger reduces the systematic error to between 7% and 15%[15].

The convolution is calculated by integrating over all possible *true* energies (t):

$$g_M(E_{\text{obs}}; \vec{\theta}, \vec{p}) = \int_{0.1E_{\text{min}}}^{\infty} f_M(t; \vec{\theta}) G(t; E_{\text{obs}}, \sigma_{\text{stat}}(t; \vec{p})) \Omega(t) dt. \quad (3)$$

Re-normalizing so that the observed energies define a p.d.f., we numerically calculate the p.d.f. to be:

$$\tilde{f}_M(E_{\text{obs}}; \vec{\theta}, \vec{p}) = \frac{g_M(E_{\text{obs}}; \vec{\theta}, \vec{p})}{\int_{E_{\text{min}}}^{\infty} g_M(y; \vec{\theta}, \vec{p}) dy}, \quad (4)$$

and we must modify the likelihood found in Eq(1) accordingly:

$$\tilde{\mathcal{L}}_M(\vec{\theta}) = \sum_{i=1}^N \ln \left\{ \tilde{f}_M(E_i; \vec{\theta}) \right\}. \quad (5)$$

By finding the parameters $\hat{\theta}$ which maximize Eq(5) we can be confident that we are accounting for the statistical uncertainty inherent in data collected by a realistic detector. To model statistical errors in our toy data set, we parameterize σ_{stat} as in Eq(2) with $p_1 = 0.15$ and $p_2 = 0$.

4 Evaluating the Fit

In this section we outline ways to evaluate the fit of a candidate model to the data set. The Kolmogorov-Smirnov statistic can be used to extract a best fit minimum energy E_{min} and, with its corresponding p -value, evaluate the “absolute goodness of fit” of a candidate model (see §4.1). The relevant question for CR physics is not whether a particular model is a good fit to the data but rather whether the flux exhibits suppression (relative to the single power-law form) at the highest energies. To address this question directly we use two statistics with well defined p -values: the Tail-Power statistic (see §4.2), which can give information about tail suppression in standard deviations, and a likelihood ratio that allows rejection of the single power-law hypothesis in favor of a suppressed candidate model (see §4.3).

4.1 Kolmogorov Statistic

While the minimum value of the likelihood function will indeed give the best value of the fit parameters, this fit may nonetheless be poor. The typical[5,4] method for evaluating goodness of fit is the Kolmogorov-Smirnov test[16]. The

relevant statistic for this test is the KS distance:

$$D_{\text{KS}}(E_{\text{min}}) = \max_{E \geq E_{\text{min}}} |F_{\text{fit}}(E) - F_{\text{data}}(E)|, \quad (6)$$

where, F_{fit} and F_{data} are the cumulative distribution functions (c.d.f.) of the best fit model and the data respectively. The maximum distance between the c.d.f.'s is taken over all energies in the fitted data set, $E \geq E_{\text{min}}$. By stepping over E_{min} and re-minimizing Eq(1) at each step to determine the best fit parameters, we can calculate D_{KS} as a function of E_{min} . The value of $\hat{\theta}_0 \equiv \hat{E}_{\text{min}}$ that minimizes D_{KS} can be taken as the best estimate of the minimum energy above which the model holds[4].

To test how well a particular model fits the data we must simulate many MC data sets drawn from the best fit model p.d.f. with the same number of events as the original data. The fraction of sets p_{KS} with D_{KS} greater than that of the data gives the suitable p -value; if $p_{\text{KS}} \ll 1$ then it is unlikely that the data are drawn from the model under consideration, and in this way the KS test statistic p_{KS} can rule out the different candidate models[4].

4.2 Tail Power Statistic

The Tail-Power (TP) statistic is similar to the KS statistic discussed above, however it has, at least, three advantages over p_{KS} when testing the power-law assumption;

- (1) The TP statistic and it's corresponding p -value p_{TP} are nearly independent of the value of the spectral index γ ,
- (2) The asymptotic behavior of the TP statistic is known, and therefore no simulations are required to calculate the corresponding p -value p_{TP} ,
- (3) If $\text{TP} > 0$ the deviation suggests flux *suppression in the tail* and if $\text{TP} < 0$ the deviation suggests flux *enhancement in the tail*[7] and
- (4) p_{TP} offers an unambiguous p -value in standard deviations.

This ‘‘measure of power-law-ness’’ has been developed and studied elsewhere (see [12,15,7]) and here we expand its use to the un-binned case.

The sample TP statistic is defined as [12]:

$$\hat{\tau}(E_{\text{min}}) = \hat{\nu}_1^2(E_{\text{min}}) - \frac{1}{2}\hat{\nu}_2(E_{\text{min}}), \quad (7)$$

where:

$$\hat{\nu}_n(E_{\text{min}}) = \frac{1}{N_{>}} \sum_{E_i > E_{\text{min}}} \ln^n \frac{E_i}{E_{\text{min}}} \quad (8)$$

and the sum is carried out over all $N_{>}$ events with energy greater than a given minimum. If the data are drawn from a pure power-law then $\hat{\tau}(E_{\min})$ will tend to zero as $N \rightarrow \infty$, regardless of the value of γ [5].

We may approximate the asymptotic joint distribution of $\hat{\nu}_1$ and $\hat{\nu}_2$ as a bivariate Gaussian $f_{\nu_1\nu_2}(\nu_1, \nu_2)$. The asymptotic mean and variance of ν_1 are $\frac{1}{\gamma-1}$ and $\frac{1}{N(\gamma-1)^2}$, and of ν_2 are $\frac{2}{(\gamma-1)^2}$ and $\frac{20}{N(\gamma-1)^4}$. The random variables ν_1 and ν_2 are highly correlated; the correlation coefficient is $\rho = \frac{2}{\sqrt{5}}$, *independent of γ* . Thus, for a given N and γ , we calculate the p.d.f. of τ to be,

$$f_{TP}(\tau; N, \gamma) = \int_{-\infty}^{\infty} f_{\nu_1\nu_2}(t, 2(t^2 - \tau))dt. \quad (9)$$

The analytic “location” $\langle\tau\rangle_{TP} \sim 0$ and “shape” $\langle\sigma_{\tau}\rangle_{TP} = \sqrt{\langle\tau^2\rangle_{TP} - \langle\tau\rangle_{TP}^2} \sim N^{-1/2}(\gamma-1)^{-2}$ parameters of this distribution are consistent with simulation generated values. We measure the p -value p_{TP} for the TP statistic in units of standardized deviation,

$$p_{TP}(E_{\min}) = \frac{\hat{\tau}(E_{\min}) - \langle\tau\rangle_{TP}}{\langle\sigma_{\tau}\rangle_{TP}}. \quad (10)$$

A spectrum with flux suppression in the tail (like that in the Fermi-like model) will result in a *positive* significance[7].

The application of Eq(10) to the toy CR data set (see §2.2) is plotted in Fig.3. The top panel shows the (pure power-law) spectral index as a function of E_{\min} . A spectral index which increases as E_{\min} increases is indicative of flux suppression. The red, left leaning hatching shows the variation of $\hat{\gamma}$ due to a $\pm 1\sigma$ *systematic* shift in the energies (see §3.2) while the opposite, blue hatching shows the *statistical* error of the estimator $\hat{\gamma}$, see §3.1. The bottom panel shows the resulting TP statistic significance $p_{TP}(E_{\min})$ in standard deviations. Notice that while the systematic errors can be significant for the measured spectral index, they do not effect the TP statistic. Since we must estimate the spectral index to compute p_{TP} , we also propagate the statistical errors on $\hat{\gamma}$ to the tail power statistic.

To test the effectiveness of this statistic, we apply it to a series of simulated data sets drawn from both the Fermi and double power-law models. For all the models we set⁴ $E_{\min} = 1.0\text{EeV}$, $\gamma = 2.75$ and either $\delta = 4.75$ or $w_c = 0.10$. We vary each characteristic cut-off energy, either E_b or $E_{\frac{1}{2}}$, in three steps $\lg(E_{\text{cut}}/E_{\min}) = 0.5, 1.0, \text{ and } 1.5$. The total number of events in the data set is varied in four steps $\lg(N) \sim 2.5, 3.0, 3.5, 4.0$. For each of these twelve sets of parameter choices we make 10^3 Monte-Carlo realizations and plot the mean and RMS of $p_{TP}(E_{\min} = 1.0)$ in Fig.4.

⁴ These values are similar to the Auger[15] and HiRes[1] best fit values.

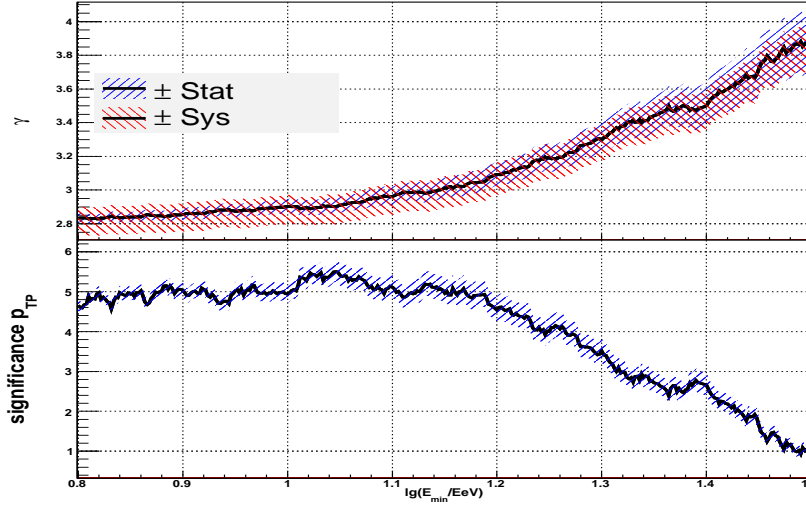


Fig. 3. *Top* The best fit (see §3.1, Eq(1)) spectral index $\hat{\gamma}$ as a function of $\lg E_{\min}$ for the toy CR data set (see §2.2) fit to the pure power-law model (P). *Bottom* The resulting TP statistic significance $p_{\text{TP}}(E_{\min})$ in standard deviations as a function of the minimum energy E_{\min} , see Eq(10). Both plots give strong evidence of flux suppression of the highest energy MC events.

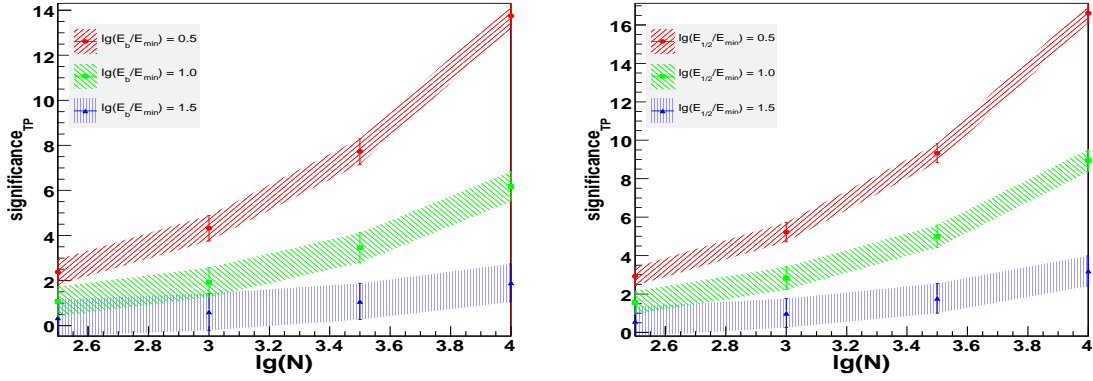


Fig. 4. The tail power significance, $p_{\text{TP}}(E_{\min} = 1.0)$ as a function of the (\log_{10} of the) number of events in each Monte-Carlo realization. Each plot style represents a different choice of $\lg(E_{\text{cut}}/E_{\min}) = 0.5, 1.0, \text{ or } 1.5$. *Left*, the double power-law, $E_{\text{cut}} \equiv E_b$. *Right*, the Fermi power-law, $E_{\text{cut}} \equiv E_{\frac{1}{2}}$.

Based on Fig.4 we can see that the best way to evaluate a data set with a potential for tail suppression is to collect as much data with E_{\min} as close to the expected cut-off as possible. The experimenter may use Fig.4, or one like it, to help tune observation parameters, i.e. collecting time on a gamma ray source or size of a CR detector, in advance of the observation and in anticipation of flux suppression of a certain type. Note, however, that one should choose

an E_{\min} *prior* to analyzing a data set to avoid a penalty for scanning in this parameter.

4.3 Model Discrimination

Here we introduce a likelihood ratio test designed to discriminate candidate suppressed models (DP and FP) from the pure power-law. We define two log-likelihood ratios; for each model M:

$$\mathcal{R}_M = \sum_{i=1}^N \{\ell_M(E_i) - \ell_P(E_i)\} = \mathcal{L}_M - \mathcal{L}_P, \quad (11)$$

where $\ell_M(E_i) = \ln f_M(E_i; \hat{\theta})$ with M either DP (double power-law) or FP (Fermi-like), and $\ell_P(E_i) = \ln f_P(E_i; \hat{\theta})$ for the pure power-law likelihood per event (see Table 1 and Eq(1)). Note that each suppressed model is fit *independently* of the pure power-law best fit. The asymptotic variance of \mathcal{R} can be estimated by the sample value:

$$\sigma_{\mathcal{R}}^2 = \frac{1}{N} \sum_{i=1}^N \left\{ [\ell_M(E_i) - \ell_P(E_i)] - \left[\frac{\mathcal{L}_M - \mathcal{L}_P}{N} \right] \right\}^2, \quad (12)$$

The hypothesis of the pure power-law is *nested* within the hypothesis of a suppressed power-law. As a consequence, $|\mathcal{R}|/\sigma_{\mathcal{R}} \rightarrow 0/0$ as $N \rightarrow \infty$ and the distribution of $\mathcal{R}/\sigma_{\mathcal{R}}$ is not Gaussian[4]. The correct p -value is calculated as the integral of a χ^2 function[14,4]:

$$p_{\mathcal{R}}(z^2) = \frac{1}{\sqrt{2\pi}} \int_{z^2}^{\infty} t^{-1/2} e^{-t/2} dt, \quad (13)$$

where $z^2 = \mathcal{R}_M^2 / (2N\sigma_{\mathcal{R}}^2)$.

We interpret this p -value in the following way: if $p_{\mathcal{R}}$ is “small” then the best fit model M may be preferred over the best fit pure power-law. By small we mean that, *a priori* and rather arbitrarily, we may choose to reject the single power-law in favor of the model if $p_{\mathcal{R}} \leq 10^{-3}$. This quantity tells us only whether a given suppressed model is better than the pure power-law. It says nothing about how well any of the fits actually represent the data.

For each of the twelve sets of parameter choices used in Fig.4, we plot the mean and RMS of $p_{\mathcal{R}}$ in Fig.5. As before, we see that the best way to reject the power-law in favor of the suppressed model is to collect as much data with E_{\min} as close to the expected cut-off as possible. Note that for $\lg(E_{\text{cut}}/E_{\min}) = 1.5$ the distribution of likelihood ratios is strictly positive and highly peaked near zero; the mean and RMS are not good reflections of this distribution.

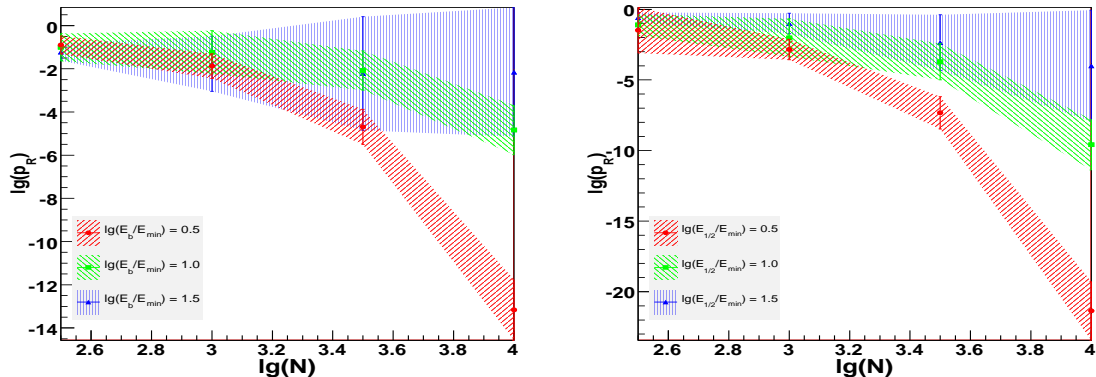


Fig. 5. The log of the likelihood ratio significance, $p_{\mathcal{R}}$ as a function of the (\log_{10} of the) number of events in each Monte-Carlo realization. Each plot style represents a different choice of $\lg(E_{\text{cut}}/E_{\text{min}}) = 0.5, 1.0, \text{ or } 1.5$. *Left*, the double power-law, $E_{\text{cut}} \equiv E_{\text{b}}$. *Right*, the Fermi power-law, $E_{\text{cut}} \equiv E_{\frac{1}{2}}$.

5 Summary and Conclusion

In this paper we describe a set of statistical tools designed to extract the most accurate and precise information about the flux of the highest energy cosmic rays. We show how to use the un-binned likelihood method described in §3.1 to fit a data set to the three model distributions described in §2.3. Techniques for incorporating the systematic and statistical errors associated with a real CR detector into the likelihood method are described in §3.2 and §3.3 respectively. In §4 we describe p -values useful for extracting information about flux suppression. We show in §4.2 and §4.3 how an experimenter might use an *a priori* estimate of the cut-off energy to maximize an observational setup for detecting flux suppression.

The collection of these statistical tools are the primary result of this paper. To answer the questions posed in the introduction for a given data set we suggest the following steps:

- (1) Estimate the best fit parameters $\hat{\theta}$ of the model;
 - (a) The estimates $\hat{\gamma}$, \hat{E}_{b} or $\hat{E}_{\frac{1}{2}}$ and $\hat{\delta}$ or \hat{w}_c are determined via the likelihood Eq(1),
 - (b) The estimate of the minimum energy E_{min} is that which minimizes the Kolmogorov distance D_{KS} (see §4.1).
- (2) Shift the energies up and down according to the systematic uncertainty described in §3.2 and repeat step (1). The resulting shift in parameter estimates gives the systematic uncertainty of those estimates.
- (3) Obtain the model parameter estimates using the methods in §3.3 to in-

corporate the statistical error of each event energy.

- (4) Test the model hypothesis;
 - (a) The absolute goodness of fit for any of the models can be evaluated using p_{KS} in §4.1,
 - (b) The Tail-Power statistic p_{TP} can be used to reject the single power-law hypothesis (nearly independently of the spectral index estimate, see §4.2)
 - (c) The single power-law may be rejected in favor of a specific alternative model using $p_{\mathcal{R}}$, here we study the double and Fermi power-law distributions (see §4.3).

The best estimates for the *characteristic cut-off energy and shape parameters*, determined via steps (1), (2) and (3), are \hat{E}_b or $\hat{E}_{\frac{1}{2}}$ and $\hat{\delta}$ or \hat{w}_c respectively. The presence of *flux suppression at the highest energies* can be evaluated using step (4).

By applying these methods to the toy Monte-Carlo set of CRPropa events we illustrate in §C how the procedure may be implemented on an actual CR detector, i.e. a detector with systematic and statistical event energies. Suppression in the tail is clear in Fig.C.1 and Fig.C.2; the tail power statistic is 4.6σ and the p -value for the double (Fermi) power-law is $\lg p_{\text{DP}} = -2.7$ ($\lg p_{\text{FP}} = -1.9$).

The methods are sufficient and robust. Indeed, many of them have been applied by the Auger collaboration which reports suppression with 6σ confidence[15]. These tools serve as a basis for further investigation of the CR spectrum such as evidence for more detailed spectral information. They can be applied to any data set, astrophysical or otherwise, to provide information both about data already collected and help to optimize future observations for detecting tail suppression.

A Binned vs. Un-Binned

The statistical superiority of an un-binned maximum likelihood estimate of the pure power-law spectral index to the logarithmically binned least- χ^2 method often used has been established in [5] and expanded upon more recently in [9,11,4,7,8]. In this section we compare the binned to the un-binned fitting method for the two suppressed models, i.e. the double and Fermi power-laws (see §2.3).

To calculate the binned estimators we minimize a $\chi^2(\vec{\theta})$ function that relates the logarithmically binned (width w) histogram of the data to that expected by a model. The function is⁵,

$$\chi^2(\vec{\theta}) = \sum_{i=1}^{N_b} \left(\frac{\lg Y_i^{\text{data}} - \lg Y_i^{\text{fit}}(\vec{\theta})}{\sigma_i^{\text{data}}} \right)^2, \quad (\text{A.1})$$

where N_b is the number of bins, Y_i^{data} is the number of events in the i^{th} bin b_i and σ_i is determined by Gaussian errors when $Y_i^{\text{data}} > 10$ and Poissonian errors when $Y_i^{\text{data}} \leq 10$. We minimize with respect to the parameters $\vec{\theta}$ (with $\theta_0 \equiv E_{\text{min}}$ fixed) using the number of events in a bin expected by the model M ,

$$Y_i^{\text{fit}}(\vec{\theta}) = N \int_{10^{b_i-w/2}}^{10^{b_i+w/2}} f_M(t; \vec{\theta}) dt.$$

To study the asymptotic bias and error produced by the two estimation techniques we draw 10^5 sets of 5×10^3 events from a pure power-law and separately from a double distribution. For each Monte-Carlo set we estimate the best fit model parameters $\hat{\theta}$ using both the likelihood Eq(1) and the χ^2 Eq(A.1) methods. The un-binned estimator of the pure power-law spectral index (see §3.1) has been shown[5,9] to have an error estimate within $\sim 1\%$ of the Cramer-Rao lower bound for a sample with as few as ~ 100 events.

In Fig.A.1 and Fig.A.2 we plot the results of the simulations. We can conclude that the un-binned fitting method is most important when fitting a power-law in the tail of a distribution; the binned estimator performs nearly as well as the un-binned for the double power-law parameters γ and E_b . The (binned) methods used to report parameters like the ‘‘ankle’’ and the ‘‘knee’’ in [15] and [1] are sufficient but limited by the bin width.

⁵ For the case of the single power-law $\lg f_P = \lg C - \gamma \lg E$ where C is the normalization. Thus the binned fitting method reduces to fitting the \log_{10} of the (error weighted) bin heights to a straight line with slope γ . This technique is often used to mitigate the effects of the heaviness of the power-law tail but un-binned methods are more accurate and precise.

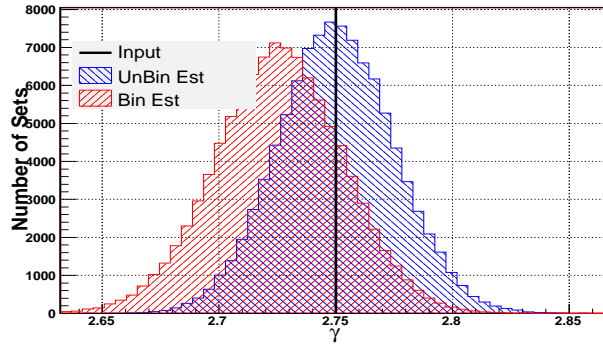


Fig. A.1. For each of 10^5 sets of 5×10^3 events drawn from a pure power-law with index $E_{\min} = 1.0$ and $\gamma = 2.75$ we estimate the spectral index using the binned Eq(A.1) and un-binned Eq(1) methods. The bias and error of the un-binned estimator is 0.0002 and 0.0247 and that of the binned is -0.024 and 0.0272.

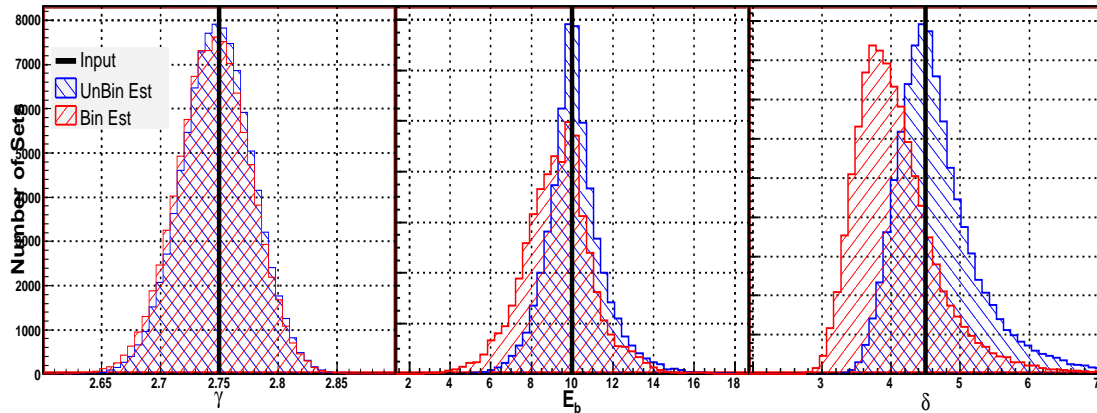


Fig. A.2. For each of 10^5 sets of 5×10^3 events drawn from a double power-law with parameters $\{\gamma, E_b, \delta\} = \{2.75, 10.0, 4.5\}$ we estimate the spectral index using the binned Eq(A.1) and un-binned Eq(1) methods. The bias and error of the un-binned estimators are $\{-0.002, 0.13, 0.16\}$ and $\{0.03, 1.4, 0.60\}$ and those of the binned are $\{-0.005, -0.71, -0.43\}$ and $\{0.03, 1.7, 0.60\}$.

B Statistical Error: Monte-Carlo Example

To illustrate the effect the statistical energy smearing has on a pure power-law we generate 9000 MC events from a power-law distribution with $E_{\min} = 1.0$ and $\gamma = 2.75$. A histogram of these events is represented by the black filled circles plotted in Fig.B.1. By minimizing Eq(1), we calculate the estimated spectral index for this data to be $\hat{\gamma} = 2.742 \pm 0.019$ (with $E_{\min}^{\hat{}} = 1.0$, see §4.1). A power-law with these parameters is plotted as the dashed line in Fig.B.1.

To each MC event E_i we then add a random number Y_i drawn from a normal distribution with mean zero and variance $0.2E_i$. The new events are histogrammed with blue open circles in Fig.B.1. We fit these events by maximizing a likelihood with

$$\int_{E_{\min}}^{\infty} f_M(t; \vec{\theta}) G(t; E_{\text{obs}}, \sigma_{\text{stat}}(t; \vec{p})) dt. \quad (\text{B.1})$$

(compare with Eq(3)) as the p.d.f. and we find that $\hat{\gamma} = 2.749 \pm 0.020$. The smearing does not effect the estimated spectral index, though it does increase the error of the estimate. The dashed curve in Fig.B.1 shows Eq(B.1) evaluated at the best fit values. Notice that the histogram of the smeared energies deviates from the un-smeared case near $\lg E \sim 0$. In §3.3 we account for this edge effect at the low energy end by assuming that the true energies follow the power-law well below the observed minimum energy; in constructing the likelihood we choose $0.1E_{\min}$ for the lower range of integration (compare Eq(B.1) with Eq(3)) and we re-normalize to ensure a true p.d.f. (see Eq(4)).

C Results of CRPropa Toy Set

By applying the statistical tools presented in this paper (summarized by steps (1)-(4)⁶ in §5) to the toy set of 5×10^3 CRPropa events (see §2.2) we illustrate how the tools might be implemented on an actual CR detector. By construction, this toy set has parameter estimates and, more importantly, errors estimates and hypothesis test p -values that are numerically comparable with those reported by Auger[15] and HiRes[1].

In preparation for this paper we generated 14 CRPropa simulations of $\sim 2 \times 10^5$ events with different injection spectral indexes, $\gamma_{\text{IN}} = (2.0, 2.1, \dots, 2.6)$, and with different values of maximum generation energy, $E_{\text{max}}/\text{EeV} = (400, 2000)$. The (after propagation) estimated characteristic break point energy, i.e. $\hat{E}_{\frac{1}{2}}$ or

⁶ Note that since we are not interested in the absolute goodness of fit for any of these *toy* models to this *toy* data set, we do not perform step (4a) of §5.

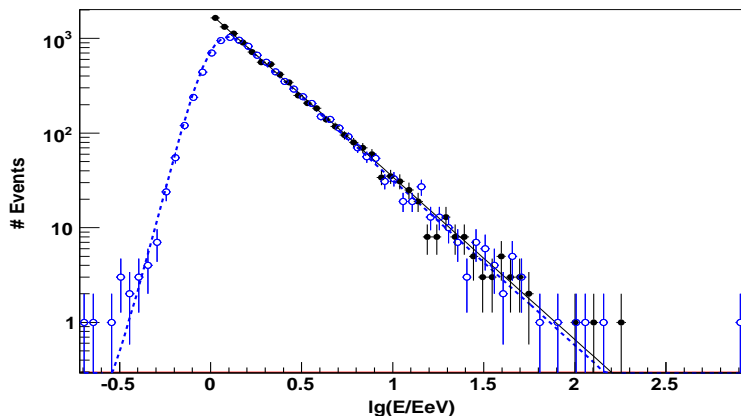


Fig. B.1. An example of a pure power-law before and after smearing. A histogram of 9000 events drawn from a single power-law with $E_{\min} = 1.0\text{EeV}$ and $\gamma = 2.75$ is plotted in black filled circles. The best fit (using Eq(1)) power-law for these events is plotted in solid black. The blue open circles are a histogram of these events after being smeared by a Gaussian with variance $0.2E$ (see §B). The blue dashed curve shows the best fit using Eq(B.1). To account for the edge effect near $\lg E \sim 0$ we use the methods in §3.3, namely Eq(3).

\hat{E}_b , is found to be independent of the spectral index at the site of generation, γ_{IN} . The estimated spectral index γ_{OUT} is found to be linearly related to the input spectral index γ_{IN} with linear slope ~ 1 . The high energy estimated shape parameters, δ and w_c , are more sensitive to the maximum generation energy (at the sources) than they are to γ_{IN} .

In Figs. C.1 and C.2 we plot the toy data set and the best fit models in two (non-binned) ways not commonly seen in the CR literature. The first is a *rank-frequency* plot. For each event (black filled circle) we plot $\lg E$ along the horizontal axis and the log of the number of events with energy greater than E along the vertical. For each of the models (see §2.3), the vertical axis is $\lg(N_{\text{tot}}(1 - F(E)))$ where $F(E)$ is the model cumulative distribution function. From the rank-frequency plot we derive an instructive visualization tool in Fig.C.2; we plot the difference between the number of events above a given energy for the toy set $N_{>}^{\text{obs}}$ and that expected by the best fit models $N_{>}^{\text{exp}}$.

The best fit pure power-law parameters for the toy set described in §2.2 are $E_{\min} = 6.31 \pm 0 \pm_{-0.82}^{0.82}$ and $\gamma = 2.83 \pm_{-0.03}^{0.03} \pm_{+0.10}^{-0.07}$ where the first error is statistical and the second systematic. The tail power significance p_{TP} is 4.6σ . The best fit double power-law parameters for the toy set are $E_{\min} = 6.31 \pm 0 \pm 0.82$, $\gamma = 2.71 \pm 0.03 \pm_{+0.10}^{-0.06}$, $E_b = 45.7 \pm_{-4.1}^{2.3} \pm 9.9$ and $\delta = 4.30 \pm 0.26 \pm_{+0.20}^{-0.11}$. The correlation coefficients are $\rho_{\gamma E_b} = 0.18$, $\rho_{\gamma \delta} = -0.15$ and $\rho_{E_b \delta} = 0.32$, see Fig.C.3. The likelihood ratio significance is $\lg p_{\mathcal{R}} = -2.7$. The best fit Fermi power-law parameters for the toy set are $E_{\min} = 6.31 \pm 0 \pm 0.82$, $\gamma = 2.69 \pm 0.03 \pm_{+0.09}^{-0.06}$,

$E_{\frac{1}{2}} = 78.6 \pm_{7.6}^{6.8} \pm_{19.1}^{18.6}$ and $w_c = 0.139 \pm_{0.029}^{0.024} \pm_{0.008}^{0.005}$. The correlation coefficients are $\rho_{\gamma E_{\frac{1}{2}}} = 0.61$, $\rho_{\gamma w_c}$ and $\rho_{E_{\frac{1}{2}} w_c} = -0.07$, see Fig.C.4. The likelihood ratio significance is $\lg p_{\mathcal{R}} = -1.9$.

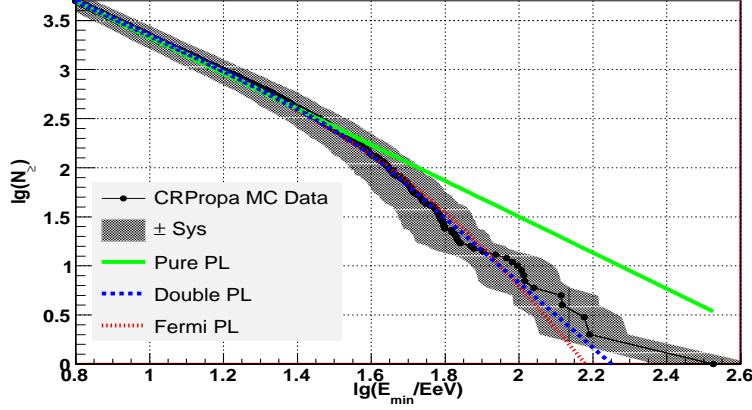


Fig. C.1. A rank-frequency plot as simulated by 5×10^3 events from the CRPropa set with parameters $\gamma_{\text{IN}} = 2.6$ and $E_{\text{max}} = 2000$ EeV. For each event (black filled circle) we plot $\lg E$ along the horizontal axis and log-number of events with energy greater than E along the vertical. The models are described in §2.3.

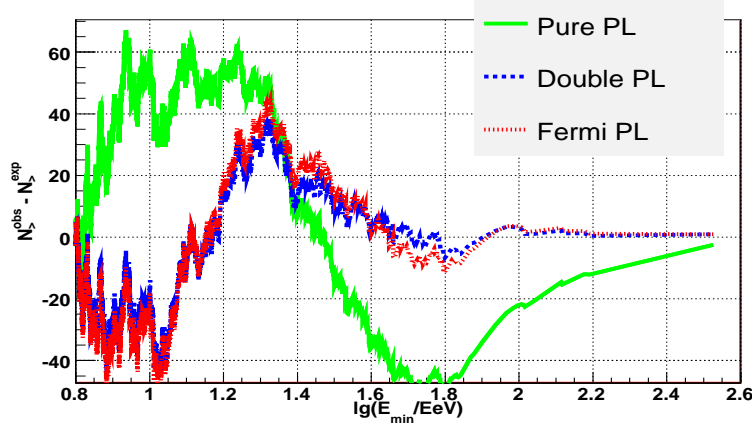


Fig. C.2. Using the rank-frequency plot (see Fig.C.1) we plot the difference between the number of events above a given energy for the toy set $N_{>}^{\text{obs}}$ and that expected by the best fit models $N_{>}^{\text{exp}}$. Note that at $\lg E_{\min}/\text{EeV} \sim 1.7$, there are at least forty fewer events observed than expected by the pure power-law fit, i.e. flux suppression.

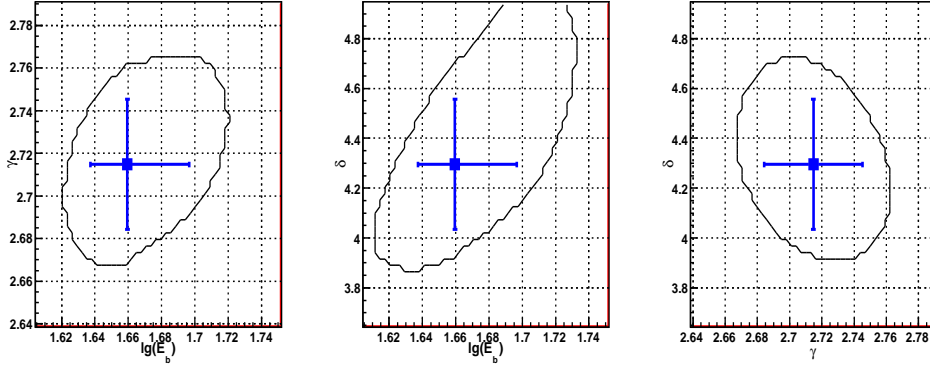


Fig. C.3. The change in log-likelihood $-2\Delta\mathcal{L}_{\text{DP}}$ (see §3.1) as a function of the parameters γ , E_b and δ of the double power-law. The data set is the toy set described in §2.2. The best estimate for each parameter is plotted as a blue box, the asymmetric one degree of freedom error estimates ($-2\Delta\mathcal{L}_{\text{DP}} = 1$) are plotted as solid blue lines and the black contour defines the two degree of freedom error estimate ($-2\Delta\mathcal{L}_{\text{DP}} \geq 2.30$).

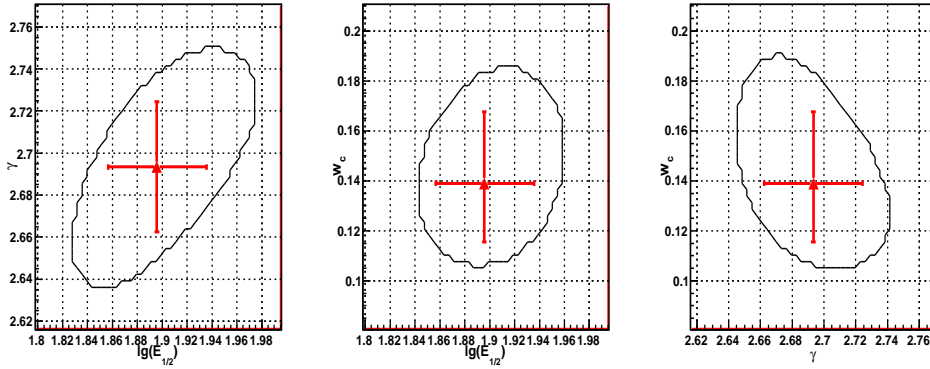


Fig. C.4. The change in log-likelihood $-2\Delta\mathcal{L}_{\text{FP}}$ (see §3.1) as a function of the parameters γ , $E_{\frac{1}{2}}$ and w_c of the Fermi power-law. The data set is the toy set described in §2.2. The best estimate for each parameter is plotted as a blue box, the asymmetric one degree of freedom error estimates ($-2\Delta\mathcal{L}_{\text{FP}} = 1$) are plotted as solid blue lines and the black contour defines the two degree of freedom error estimate ($-2\Delta\mathcal{L}_{\text{FP}} \geq 2.30$).

References

- [1] R. Abbasi et al. Observation of the GZK cutoff by the HiRes experiment. *Phys. Rev. Lett.*, 100:101101, 2008.
- [2] Eric Armengaud, Gunter Sigl, Tristan Beau, and Francesco Miniati. CRPropa: A numerical tool for the propagation of UHE cosmic rays, gamma-rays and neutrinos. *Astropart. Phys.*, 28:463–471, 2007.
- [3] V. S. Berezinsky and S. I. Grigorieva. *Astro. and Astrophys.*, 199(1), 1988.
- [4] A. Clauset, C.R. Shalizi, and E.J. Newman. Power-law Distributions in Empirical Data, 2007. arXiv:0706.1062v1.
- [5] M. L. Goldstein, S. A. Morris, and G. G. Yen. Problems with fitting to the power-law distribution. *The European Physical Journal B - Condensed Matter and Complex Systems*, 41(2):255–258, 2004.
- [6] Kenneth Greisen. End to the cosmic-ray spectrum? *Phys. Rev. Lett.*, 16(17):748–750, Apr 1966.
- [7] J. D. Hague, B. R. Becker, M. S. Gold, and J. A. J. Matthews. Power Laws and the Cosmic Ray Energy Spectrum. *Astropart. Phys.*, 27:455–464, 2007.
- [8] J. D. Hague, Bernard Raymond Becker, Michael S. Gold, J. A. J. Matthews, and J. Urbar. Statistical Methods for Investigating the Cosmic Ray Energy Spectrum. *ICRC-07 Abs.Num.1217*, 2007.
- [9] L. W. Howell. Statistical Properties of Maximum Likelihood Estimators of Power Law Spectra Information. *NASA/TP-2002-212020/REV1, Marshall Space Flight Center*, 2002. <http://www.sti.nasa.gov>.
- [10] F. James and M. Roos. Minuit: A System for Function Minimization and Analysis of the Parameter Errors and Correlations. *Comput. Phys. Commun.*, 10:343–367, 1975. We use the CERN root-systems v5.1 implementation available at <http://www.root.org>.
- [11] M. E. J. Newman. Power Laws, Pareto distributions and Zipf’s Law. *Contemporary Physics*, 46:323–351, 2005.
- [12] V. Pisarenko, D. Sornette, and M. Rodkin. Deviations of the Distributions of Seismic Energies from the Gutenberg-Richter Law. *Computational Seismology*, 35:138–159, 2004.
- [13] M. Schroedter et. al. A Very High Energy Gamma-Ray Spectrum of 1ES 2344+514. *arXiv*, 2005. arXiv:astro-ph/0508499v1.
- [14] Quang H. Vuong. Likelihood ratio tests for model selection and non-nested hypotheses. *Econometrica*, 57(2):307–333, 1989.
- [15] T. Yamamoto et al. The UHECR spectrum measured at the Pierre Auger Observatory and its astrophysical implications. 2007. [http://www.auger.org/technical info/pdfs/icrc2007/0707.2638v1.pdf](http://www.auger.org/technical%20info/pdfs/icrc2007/0707.2638v1.pdf).

- [16] W. M. et. al. Yao. Review of Particle Physics. *Journal of Physics G*, 33:1+, 2006.
- [17] G. T. Zatsepin and V. A. Kuzmin. Upper limit of the spectrum of cosmic rays. *JETP Lett.*, 4:78–80, 1966.
- [18] I. Zehavi et. al. On Departures From a Power Law in the Galaxy Correlation Function. *arXiv*, 2005. arXiv:astro-ph/0508499v1.